Modification of Titan's ion tail and the Kronian magnetosphere: Coupled magnetospheric simulations

R. M. Winglee,[1] D. Snowden,[1] and A. Kidder[1]

Received 23 April 2008; revised 8 February 2009; accepted 3 March 2009; published 23 May 2009.

[1] Three-dimensional multifluid/multiscale modeling is used to study the coupled interaction between the Kronian magnetosphere and Titan's induced magnetosphere. The multifluid aspect of the model allows ions from the solar wind, Saturn's ionosphere, Enceladus torus, and Titan's ionosphere to be tracked separately. The multiscale aspect of the model allows simultaneous resolution of global and local processes down to 100 km near Titan. In the simulation, Titan is placed in the premidnight sector at 2100 Saturn local time. Two orientations of interplanetary magnetic field (IMF) are considered: parallel and antiparallel to Saturn's planetary field. During parallel IMF, plasma conditions near Titan are relatively stable and Titan's ion tail extends to 10 Saturn radii. The ion tail produces mass loading of the Kronian plasma disk and leads to a modification of the position of the plasma sheet. During antiparallel IMF, fingers of cold dense plasma from the inner magnetosphere propagate outward, driven by the centrifugal interchange instability. Titan's interaction with the fingers causes enhanced outflow as well as large changes in the orientation of Titan's ion tail. The plasma fingers are also disrupted by the interaction with Titan. In both IMF configurations, ions lost from Titan do not produce a complete ion torus. However, Titan's ion tail has global importance because it influences the inner boundary of the plasma sheet and has the potential to modify Kronian auroral processes when it is in this position in the Kronian magnetosphere.

Citation: Winglee, R. M., D. Snowden, and A. Kidder (2009), Modification of Titan's ion tail and the Kronian magnetosphere: Coupled magnetospheric simulations, *J. Geophys. Res.*, *114*, A05215, doi:10.1029/2008JA013343.

1. Introduction

[2] Cassini has confirmed that Saturn has a highly variable and complex magnetosphere that is influenced by planetary rotation, internal plasma sources, the solar wind and the interplanetary magnetic field [*Dougherty et al.*, 2005; *Crary et al.*, 2005; *Young et al.*, 2005]. The internal plasma sources not only include the Kronian ionosphere and rings but also from its moons including Enceladus [*Young et al.*, 2005] and Titan [*Wahlund et al.*, 2005]. Planetary rotation is the primary source of energization of the plasma within about 16–18 R_S (where 1 R_S is Saturn radius equal to 60,268 km) [*Krupp*, 2005] but like the terrestrial magnetosphere it is strongly modified by the direction of the interplanetary magnetic field (IMF) [*Hansen et al.*, 2000, 2005] and by pressure pulses in the solar wind [*Crary et al.*, 2005]. Variations as much as 20 R_S in the position of the bow shock and magnetopause have been observed by different spacecraft flybys [*Blanc et al.*, 2002; *Hendricks et al.*, 2005].

[3] Current models for the Saturn/Titan system fall into one of two types: global models of Saturn's magnetosphere, and local models of Titan's magnetosphere induced by the flow of Kronian plasma passed Titan. Fluid simulations of Saturn include MHD models and multifluid models. MHD models [*Hansen et al.*, 2000, 2005], which neglect the presence of moons and treat the plasma with a single fluid, have demonstrated the importance of IMF conditions in modifying the shape of the magnetosphere, including the magnetic field structure and plasma flows within it. Multifluid simulations include light solar wind protons and heavy (water group) and light (protons) ions from the Kronian ionosphere and Enceladus [*Kidder et al.*, 2009]. Multifluid simulations demonstrate that enhanced convection of plasma from Enceladus (owing to either an increased convective electric field from antiparallel IMF or increased outflow from an Enceladus plume) leads to a centrifugal interchange instability. This instability causes heavy ions that originate from Enceladus to move outward while hotter but more tenuous solar wind plasma is drawn inward, leading to the formation of discrete interchanging fingers of plasma.

[4] Local simulations of just Titan are frequently modeled by MHD [*Nagy et al.*, 2001; *Kopp and Ip*, 2001; *Ma et al.*, 2004], hybrid [*Brecht et al.*, 2000; *Ledvina et al.*, 2004; *Simon et al.*, 2007], or multifluid codes [*Snowden et al.*, 2007]. In these simulations Saturn's magnetospheric conditions near Titan are assumed and held constant and the modification to the Titan environment is then calculated, but any influences of Titan on the Kronian magnetosphere (e.g., lobe or plasma sheet) are not explicitly addressed. Several models have studied the interaction at Titan at different

[1]Department of Earth and Space Science, University of Washington, Seattle, Washington, USA.

0148-0227/09/2008JA013343

Saturn local times (SLT) [*Brecht et al.*, 2000; *Simon et al.*, 2007] or in the magnetosheath [*Ledvina et al.*, 2004; *Simon et al.*, 2007]. However, these simulations assume uniform spatial and temporal conditions within Saturn's magnetosphere and only adjust the properties of Titan's ionosphere owing to changes in solar illumination. It has been shown that the interaction with the hotter plasma in the magnetosheath can have a significant effect on the formation of boundary layers and the acceleration of plasma from Titan [*Ledvina et al.*, 2004; *Simon et al.*, 2007]. *Snowden et al.* [2007] have shown, using multifluid simulations, that Titan's ion tail with densities above the incident Kronian plasma density could extend to least a few Saturn radii in length, suggesting that it may be large enough to have a significant effect on the Kronian magnetosphere.

[5] Coupling these two systems is difficult owing to the disparate time and length scales involved in accurately modeling the influence that Titan's induced magnetosphere and Saturn's magnetosphere exert on one another. However, if model results are correct that Titan's ion tail is at least a few Saturn radii in length, its impact on the Kronian magnetosphere may not be negligible. Similarly, it is unknown how temporal variations in Kronian conditions affect the transport of plasma from Titan. The importance of this task is demonstrated by *Menietti et al.* [2007] who have shown that Titan may modify Saturn kilometric radiation (SKR). According to their study the occurrence of SKR increases when Titan is in the magnetotail and decreases when Titan is near noon SLT. These results imply that Titan's modification of the Kronian magnetosphere has global consequences.

[6] We present results from a three-dimensional multifluid/multiscale model that addresses the coupling of moon/planet plasma interactions. The details of the model are given in section 2. The multiscale aspect allows for the resolution of Titan's induced magnetosphere, Saturn's global magnetosphere and the coupling between these two systems. The multifluid component allows us to track the transport of different ion species in these systems. In this simulation Titan is placed in the premidnight sector (2100 SLT). Two configurations of the IMF (parallel and antiparallel to the planetary magnetic field at the magnetopause) are used to demonstrate how the variability of Saturn's magnetosphere affects Titan and how Titan in turn exerts control on some aspects of Saturn's magnetosphere. These simulations are the first of their type and allow us to examine Titan's interaction over several hours as opposed to a few tens of minutes that local simulations are typically restricted to. Future work needs to expand these simulations to tens of hours to fully examine the fate of Titan's plasmas within the Kronian magnetosphere. Neutral/plasma interactions are probably important very close to Saturn's satellites and rings. The interactions considered here model the more distant interactions so that neutral/plasma interactions are not included in the present model. The local Kronian and Titan plasma environment are described in section 3. For parallel IMF, we observe that Titan's ion tail is relatively stable, but spirals inward so that a closed torus is not produced. For antiparallel IMF the outflow rate from Titan is seen to increase and its ion tail is shown to undergo flapping. Both effects arise from the changes in the local Kronian magnetosphere conditions. The effects of the coupled systems are described in section 4 when intermediate and large-scale views of the systems are examined. These views show the disruption of the plasma fingers for the antiparallel case and this disruption leads to the generation of detached plasma blobs. Section 5 gives examples of effects that Titan's ion tail has on the Kronian magnetosphere. These effects include the change in position of the plasma disk during parallel IMF and modified plasma flows at the inner edge of the Kronian plasma sheet during antiparallel IMF. A summary of results is given in section 6.

2. Model

2.1. Multifluid Equations

[7] In order to accurately model the coupling of the Kronian magnetosphere and Titan's induced magnetosphere, one must incorporate ion dynamics from the different sources of plasma (solar wind, Saturn, Enceladus and Titan). It is necessary to go beyond MHD, which is a single-fluid model, and include multiple ion populations with individual temperatures and velocities for each species. This technique originally developed for magnetospheric applications [*Winglee*, 1998, 2000, 2004] has been successfully used to model ion cyclotron and ion skin depth effects within weakly magnetized systems such as Mars and Ganymede [*Harnett and Winglee*, 2003, 2007; *Paty and Winglee*, 2004, 2006], and the pickup of heavy ions [*Harnett et al.*, 2005]. The model is also able to differentiate heavy and light ion physics, such as in the development of the interchange instability at Saturn [*Kidder et al.*, 2009].

[8] The multifluid code fully incorporates ion skin depth effects in Ohm's law and ion cyclotron terms in the momentum equation that can lead to the differential acceleration of different ion species. The dynamics of each plasma component is described by conservation equations for mass, momentum and pressure given by

$$\frac{\partial \rho_\alpha}{\partial t} + \nabla \cdot (\rho_\alpha \boldsymbol{V}_\alpha) = 0 \tag{1}$$

$$\rho_\alpha \frac{d\boldsymbol{V}_\alpha}{dt} = q_\alpha n_\alpha (\boldsymbol{E} + \boldsymbol{V}_\alpha \times \boldsymbol{B}) - \nabla P_\alpha - \left(\frac{GM}{R^2}\right)\rho_\alpha \vec{\boldsymbol{r}} \tag{2}$$

$$\frac{\partial P_\alpha}{\partial t} = -\gamma \nabla \cdot (P_\alpha \boldsymbol{V}_\alpha) + (\gamma - 1)\boldsymbol{V}_\alpha \cdot \boldsymbol{\nabla} P_\alpha, \tag{3}$$

where the subscript α denotes the ion and electron components that constitute the plasma. In hybrid codes, and in the multifluid code, one makes the assumption that the electrons are a fluid and have sufficiently high mobility along the field lines such that they are approximately in steady state (i.e., $dv_e/dt = 0$), or in drift motion. This assumption removes high-frequency plasma and electron waves, and enables the momentum equation for the electrons to be reduced to

$$\boldsymbol{E} + \boldsymbol{V}_e \times \boldsymbol{B} + \frac{\boldsymbol{\nabla} P_e}{e n_e} = 0. \tag{4}$$

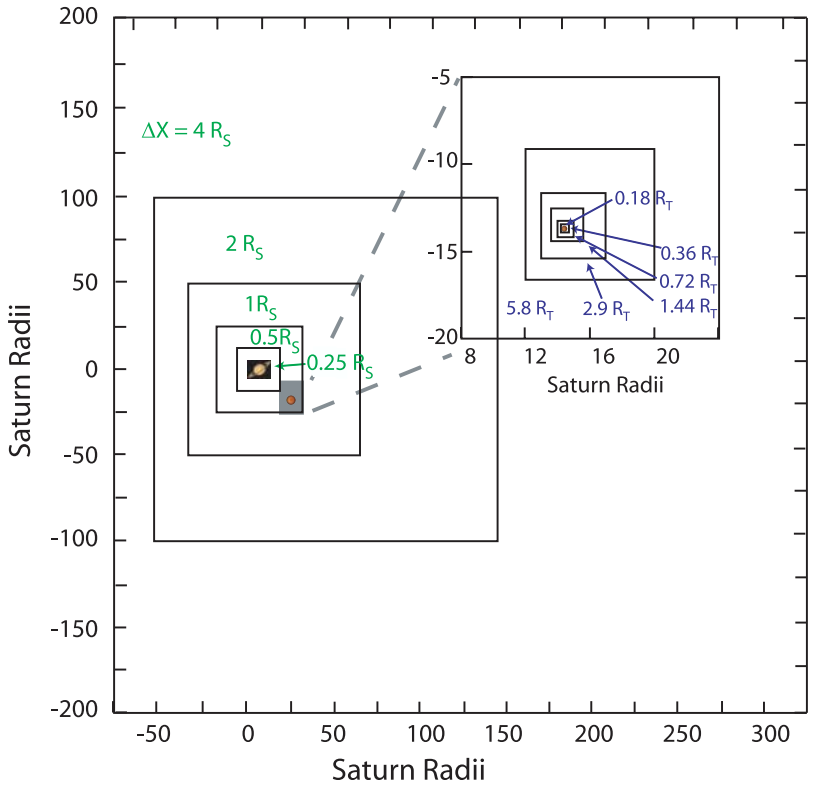

Figure 1. Nested-grid system that incorporates both Saturn's magnetosphere and Titan's induced magnetosphere. Numbers inside boxes indicate the resolution.

The electron dynamics are completed by assuming quasi-neutrality, and applying the definitions for current and electron pressure. For a single component plasma one obtains

$$N_e = N_i, \quad \boldsymbol{V}_e = \boldsymbol{V}_i - \frac{\boldsymbol{J}}{\mathrm{eN_e}}, \quad \boldsymbol{J} = \frac{1}{\mu_0}\nabla \times \boldsymbol{B} \tag{5}$$

$$\frac{\partial P_e}{\partial t} = -\gamma \nabla \cdot (P_e \boldsymbol{V}_e) + (\gamma - 1)\boldsymbol{V}_e \cdot \nabla P_e. \tag{6}$$

In the presence of multiple ion populations, (5) becomes

$$n_e = \sum_i n_i, \quad \boldsymbol{V}_e = \sum_i \frac{n_i}{n_e}\boldsymbol{V}_i - \frac{\boldsymbol{J}}{\mathrm{en_e}}, \quad \boldsymbol{J} = \frac{1}{\mu_0}\nabla \times \boldsymbol{B}. \tag{7}$$

Substitution of equation (9) into equation (4) yields a modified Ohm's law of

$$\boldsymbol{E} = -\sum_i \frac{n_i}{n_e}\boldsymbol{V}_i \times \boldsymbol{B} + \frac{\boldsymbol{J} \times \boldsymbol{B}}{en_e} - \frac{1}{en_e}\nabla P_e + \eta(x)\boldsymbol{J}. \tag{8}$$

The first term in equation (8), when assuming a single ion species, collapses into the ideal Ohm's law. The last term, $\eta(\boldsymbol{x})\boldsymbol{J}$, is added to allow for finite conductivity in the ionosphere only. Collisions beyond this region are assumed to be negligible. No anomalous resistivity is included in the code.

[9] The second and third terms in equation (8) are the Hall and Grad P_e corrections and become significant when the ion skin depth becomes comparable to the scale length of gradients. Such effects are important in determining the plasma dynamics at Titan, and with the use of localized refinement gridding described below and in Figure 1 these effects are incorporated in the present model. Ion cyclotron terms can be derived from the full momentum equation and the modified Ohm's law given by equation (8). Thus, the above equations incorporate key particle effects provide the particle distributions have approximately Maxwellian distributions.

[10] The evolution of the magnetic field is determined by the induction equation

$$\frac{\partial \boldsymbol{B}}{\partial t} + \nabla \times \boldsymbol{E} = 0, \tag{9}$$

where the electric field given by the modified Ohm's law in equation (8). Substitution of equation (8) into the ion momentum equation (2). Note also that each ion species contributes to the electric field in equation (8) which produces coupling between the species. These equations are more complicated than the MHD equations and no simple conservative form of the equations exist because of the coupling. Nevertheless, convergent solutions are easily obtained using standard techniques. The above equations are solved using a second-order Runge-Kutta method.

[11] To couple the systems, a grid system for Titan's induced magnetosphere is included within the grid system for Saturn's magnetosphere. This is accomplished by first

establishing a global equilibrium, obtained by running the Saturn simulation (with grid resolution of 0.25 R_S and an inner boundary of 2.25 R_S) for several tens of hours. When an equilibrium solution is obtained, refinement gridding, as shown in Figure 1, is applied around Titan's location specified along its orbital path, with resolution down to a few hundred kilometers. The refinement gridding continues outward to cover several Saturn radii, until it merges smoothly into the magnetospheric grid system. Plasma and field quantities are passed between grid systems at each time step, ensuring full coupling. By coupling a planetary magnetosphere with the induced magnetosphere around a moon, the multifluid/multiscale model enables the study of multiple plasma interactions in upstream and downstream directions at small and large scales for the first time.

2.2. Model Parameters

[12] The model for Saturn's magnetosphere is the same as that used by *Kidder et al.* [2008] to study the development of the centrifugal interchange cycle driven by plasma from Enceladus. The model includes one electron component (whose dynamics is determined by equations (5)–(8)) and three ion components (controlled by equations (1)–(3)). These ion components include (1) protons which can originate from the solar wind and/or the planetary/moon ionosphere; (2) moderately heavy ions such as O^+, N^+, OH^+, H_2O^+ or CH_4^+ (with an assumed overall mass of 16 amu), hereinafter referred to as the CNO^+ group; and (3) the heavy ions such as N_2^+ and O_2^+ (with an assumed mass of 32 amu), hereafter referred to as the heavy ion group (Hvy^+). The latter two ions species have either the Enceladus torus or Titan as their source. The Enceladus ion source is incorporated in the model by placing an ion torus with a density of 2 cm^{-3} CNO^+ ions at Enceladus' orbit, consistent with observations [*Young et al.*, 2005]. The plasma torus is initialized on field lines that enclose Enceladus' L-shell at 4 ± 0.5. This yields an extended torus that would be associated with ionization of neutrals well away from Enceladus. Heavy ions are initialized in this region as a tracer ion species with a density of 0.25/cm^3 [*Young et al.*, 2005]. The density derived from this initialization is held fixed at the points where the torus intersects the inner boundary. Enhanced convection rate produced by antiparallel IMF can lead to overall increases in the torus density while parallel IMF can lead to a smaller and more confined plasma torus [*Kidder et al.*, 2009] so that conditions in the inner magnetosphere can be very dynamic.

[13] An H^+ ionosphere is assumed at the inner boundary of 2.25 R_S, representing Saturn's ionosphere, and the inner boundary of the simulations. At smaller radial distances, collisional effects and ring dynamics would have to be included which is beyond the scope of the present model. This density is held constant at a value of 50 cm^{-3}. All ion fluids have a Maxwellian distribution.

[14] With Titan's thick atmosphere there are substantial collisional effects at lower altitudes below 1.5 R_T (1 R_T = 2575 km) where the plasma is approximately collisionless. Because the code does not include these collisional processes, we set the inner boundary at Titan to be 1.5 R_T presenting the topside ionosphere for the moon. At the boundary the density of CNO^+ and Hvy^+ is set to 400 particles/cm^3, with the proton density set at 200 particles/cm^3. The temperatures of Saturn and Titan's ionospheres are assumed to be low at ~1 eV. Ion outflow is achieved by induced electric fields associated with the convection of magnetic field through either system. These parameters are similar to those used in the local model of Titan developed by *Snowden et al.* [2007], and the development of the induced magnetosphere is very similar to that derived by *Snowden et al.* [2007] over the period covered in local model. This temperature is colder that Titan's actual ionosphere [e.g., *Cravens*, 2005] but the interaction with the Kronian magnetosphere leads to its heating to the observed temperature of about 100 eV. Since the derived outflows are comparable to observed outflow rates it means that the interaction with the Kronian magnetosphere is the main driver of the outflows and it is not a simple thermal wind from Titan.

[15] The Cartesian coordinate system is such that Saturn's rotation axis is in the z-direction and the negative x axis is pointed to the Sun, with the Sun being in the x−z plane though it is below the equatorial plane of Saturn. Titan is placed in the x−y plane at [14.14, −14.14, 0] R_S, i.e., in the premidnight sector. This orbital position allows us to study the flow of Titan's plasma tail into Saturn's plasma sheet. Because Saturn's rotation axis is tilted relative to its orbital plane, the solar wind is incident at an upward angle of 28° with a velocity of 400 km/s and a density of 0.05 cm^{-3}.

[16] The equilibrium for Saturn's magnetosphere is established by running the simulations for 30 hours under the above conditions, which provides for a full transit of the solar wind across the entire simulation system. This timescale is sufficiently large for the bulk of the magnetosphere to be in equilibrium with the imposed solar wind conditions Parallel IMF with a magnitude of 0.3 nT is imposed on the solar wind boundary and allowed to convected into the system and modify the configuration of the magnetosphere [cf. *Kidder et al.*, 2009]. The simulations are run for another 20 hours (i.e., between $30 < t < 50$ hours) which allows for full penetration of the solar wind electric fields into the Kronian magnetosphere and allows the latter to reconfigure and come into approximate equilibrium. At the end of this 20-hour period the IMF is turned to antiparallel with a strength of 0.3 nT and the system then run for another 20 hours (i.e., between $50 < t < 70$ hours.). Titan is inserted with the refinement gridding at $t = 38.75$ hours for the parallel case and run for approximately 5 hours. We repeat this approach for the antiparallel case except that Titan is inserted with the refinement gridding into the coarse simulations at $t = 64$ hours when the effects of antiparallel effects have penetrated into the Kronian plasma.

[17] This insertion technique allows the fate of the plasma from Titan to be tracked in the Kronian magnetosphere. In reality one would like to track the interaction across periods of several tens of hours so that full interaction over multiple rotations could be evaluated. Unfortunately, we do not have the computational resources available at this time. The insertion is in many ways very similar to the startup of a local code where the plasma is allowed to flow in from one boundary to set up a magnetosphere, except instead of vacuum the insertion occurs within an existing magnetosphere. Inspection of the early evolution of the induced magnetosphere shows that it is very similar to that obtained from local simulations. Any transients associated with the

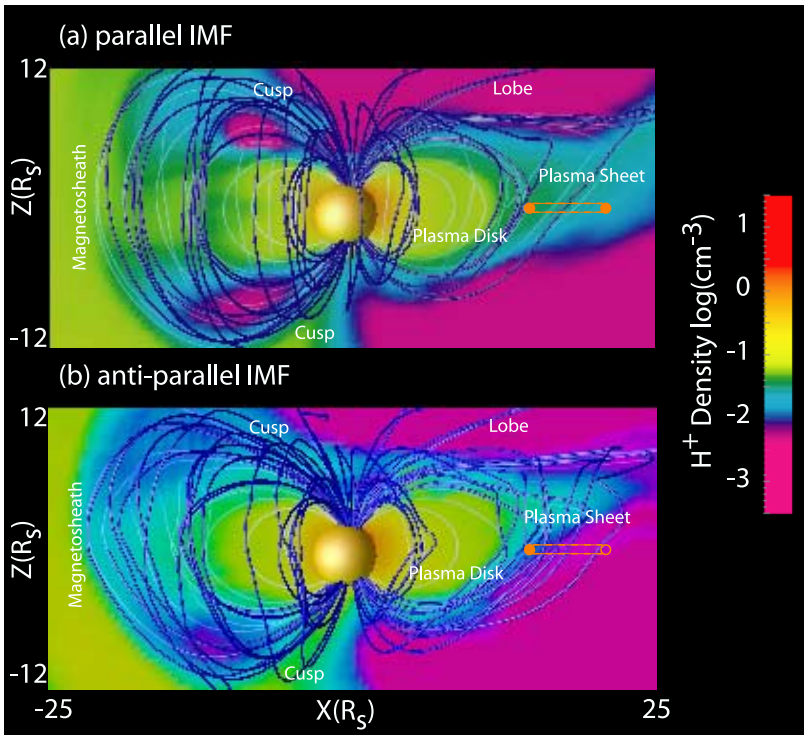

Figure 2. Initial configuration of Saturn's magnetosphere (light ion density in the noon-midnight meridian) at the time Titan's refinement grid was inserted at (a) t = 39 hours for parallel IMF (−0.3 nT) and (b) t = 64 hours for antiparallel IMF (+0.3 nT). In this image, Titan would only be a small speck if plotted to scale. To more clearly identify its position, we use a solid circle that is not to scale. Titan's ion tail, if it were fully corotated, is indicated by the dashed lines as seen from the side, with the open circle indicating its position at midnight.

injection die away within a few minutes, which is very much shorter than the few hours considered here.

[18] Another reason for limiting the length of the simulations is that the simulations neglect the orbital speed of Titan, which reflects the fact that Titan's orbital speed is very much less than the speed of the plasma at Titan's orbit. This assumption is valid if Titan's plasma does not spiral around on itself, and if Titan's orbital displacement is much smaller than Titan's ion tail. These assumptions are valid here because within 5 hours of the simulations, Saturn does a half rotation and as shown in the following Titan's ion tail appears as a distinct object out to about 90° in longitude, while Titan moves only about 5° in longitude. Further advances in computers and techniques may allow a continuous simulation over longer durations in near future but this is beyond the scope of this first paper of the coupled system. At this time there does not appear to be any observational evidence that Titan's plasma is able to form a complete torus so the above assumptions are appropriate for a first step. The model results also confirm the inability to form a complete torus.

3. Local Plasma Environments

3.1. Titan's Plasma Environment Within the Kronian Magnetosphere

[19] The Kronian plasma environment at Titan is highly variable, depending both on solar wind conditions and mass loading from the Enceladus plasma torus. Large-scale differences in the Kronian magnetosphere for parallel and antiparallel IMF are illustrated in Figure 2, which shows the density of the light ions in the noon-midnight meridian just prior to the insertion of Titan into the coupled model. In this figure several features of Saturn's magnetosphere can be identified near Titan. The bulk of the plasma in the magnetosphere lies in the plasma disk, which is identified by cold, dense plasma and is confined by closed magnetic field lines (shown in magenta) and is rotational with Saturn's magnetic field. More tenuous, hotter plasma escaping out the tail forms the plasma sheet. The very low-density regions above and below the plasma sheet are the lobes. In both cases the solar wind has direct access to the southern polar region so that there is asymmetric mass loading between the northern and southern cusps. This asymmetric loading causes the magnetosphere to be pushed upward, giving it a bowl shape [*Kidder et al.*, 2009].

[20] The projected position of Titan at 2100 SLT is indicated by the red dot. The orbital path is indicated by the dashed line, with the open circle showing Titan's position at 0000 SLT. For both parallel and antiparallel IMF, Titan is near the boundary between the cold, dense plasma disk and the tenuous, hot plasma sheet. The plasma sheet is much fatter for parallel IMF and Titan never enters the low-density lobes. For antiparallel IMF the plasma sheet is much thinner and Titan can drop out of the plasma sheet

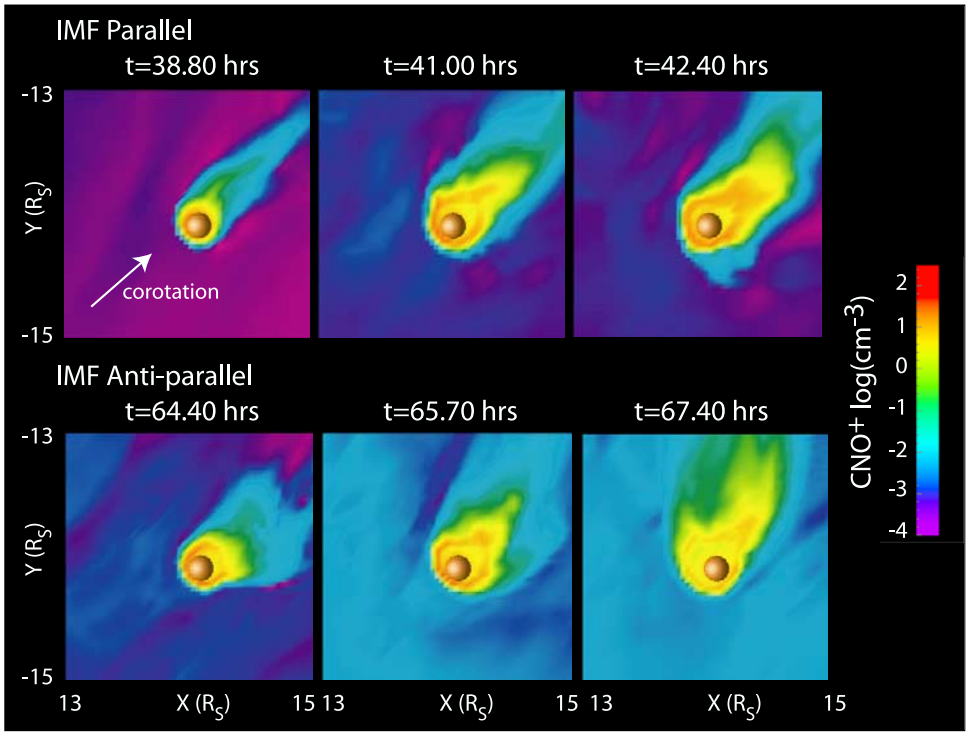

Figure 3. Evolution of the heavy ion density in the vicinity of Titan for (top panels) parallel IMF and (bottom panels) antiparallel IMF. The tail thickness and direction varies with IMF direction and in time as the local plasma conditions change.

and lie in the lobe. If Titan's beginning position were assumed to be midnight SLT, Titan would actually appear in the lobe.

3.2. Development of Titan's Ion Tail During Parallel and Antiparallel IMF

[21] Figure 3 shows the development of Titan's ion tail for parallel and antiparallel IMF in the orbital plane at mesoscales with a field of view of 2×2 R_S. Ion outflow is notably different in each case owing to the differences in the local plasma environment. For parallel IMF (top panels), a long thin tail is produced, similar to the local model of *Snowden et al.* [2007]. The ion tail grows in the direction of the incident Kronian plasma flow, which is in the direction of corotation. The direction of Titan's tail remains roughly fixed for the duration of the simulation, though the tail thickens owing to changes in local plasma conditions. The total ion loss rate is $3-4 \times 10^{24}$ ions/s with about 2.0×10^{24} protons/s, 4.0×10^{23} CNO^+/s and 7.0×10^{23} Hvy^+/s.

[22] For the antiparallel case, Titan's ion tail is nearly twice as wide and has slightly enhanced densities (lower panels of Figure 3). Thus the antiparallel case produces conditions for enhanced loss from Titan. The total ion loss rate is ~3 times higher at 1.2×10^{25} ions/s. While all ion species experience enhanced loss, CNO^+ and Hvy^+ loss rates are preferentially affected. For the light ions we see a factor of 2 increase yielding a total flux of 6.3×10^{24} protons/s. The loss rate of heavier ions increases by more than a factor of five with rates of 2.4×10^{24} CNO^+/s and 4.4×10^{24} Hvy^+/s. The ion loss rate in our simulation is consistent with the loss rate estimated from Cassini observations (~10^{25} ions/s) and with local simulations of Titan's induced magnetosphere [*Wahlund et al.*, 2005; *Snowden et al.*, 2007]. Note that the boundary conditions for Titan is the same between the two cases so that the changes in outflow is explicitly owing to the changes in forcing from the Kronian magnetosphere in response to changes in the solar wind conditions.

[23] Another important difference is that for antiparallel IMF the tail undergoes flapping (i.e., it changes direction). For example at t = 64.40 hours, the tail is on average in the corotation direction. At t = 67.40 hours, the tail swings by ~45° Saturn-ward. The fact that this flapping occurs when no flapping is seen at the same time from insertion for the parallel IMF case implies that this tail flapping is not a Titan effect but rather arises from variability within the Kronian magnetosphere. To determine why the ion tail is stable under one condition and subject to flapping under other conditions we next investigate large views of the system.

4. Coupled Plasma Interactions

4.1. An Extended Ion Tail for Parallel IMF

[24] An understanding of the coupled nature of the system can be understood through views of the plasma conditions at different scales. For parallel IMF, the lack of strong variability in the Kronian plasma near Titan enables it to grow to nearly 10 R_S. This tail, illustrated in Figure 4, shows the evolution of the 0.01 cm^{-3} surface (blue) of constant Hvy^+ density for a 16×15 R_S field of view in the equatorial plane. The white lines are streamlines indicating the flow of Kronian plasma with red lines to highlight flows that intercept Titan or its fully developed tail. The Hvy^+ plasma of the inner magnetosphere can be seen and is

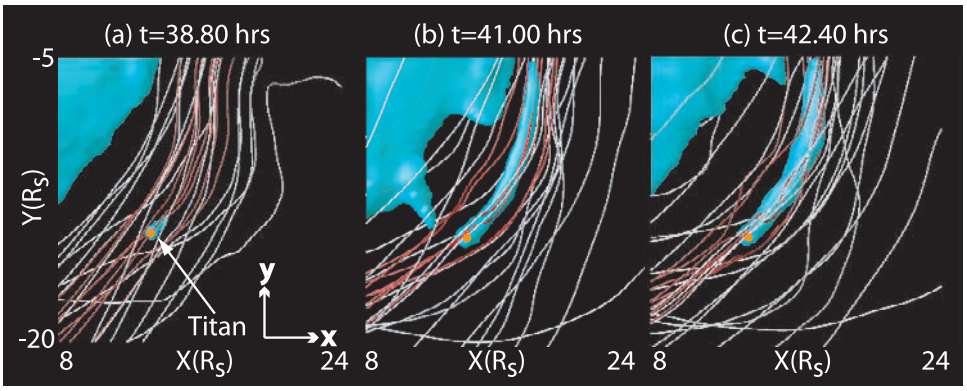

Figure 4. Surface of constant density (10^{-2} cm^{-3}) for heavy ion density (blue) for the parallel IMF case. White lines show the plasma streamlines derived from the total plasma velocity in the vicinity of Titan. The red lines highlight flows that directly interact with Titan and its ion tail. The ion tail closely tracks the streamlines and, as a result, the ion tail remains intact for ~10 R_S.

distinct from Titan's tail plasma. After a couple of hours, the ion tail reaches an approximate equilibrium extending nearly 10 R_S from Titan, with little change seen between the times shown in Figures 4b and 4c. Thus, the limited period of 5 hours for the simulations is probably appropriate, and changes in the solar wind conditions are likely to play an important role on longer timescales, as we will see when the antiparallel IMF case is considered.

[25] Saturn's plasma flows are approximately corotational along the dusk flank, but the flow becomes directed toward the planet as one moves closer to the noon-midnight meridian. This change in flow exists prior to the propagation of the tail to the region (Figure 4a) so Titan does not produce it. This magnetospheric flow causes Titan's plasma tail to bend inward and eventually intercept the dense plasma disk. As a result of this deflection, it appears difficult for Titan to generate a complete torus.

[26] A global perspective of Titan's ion tail during parallel IMF is shown in Figure 5, which shows Hvy^+ density in the equatorial plane. The black and white circles indicate positions at r = 14 and 20 R_S, respectively. The tail seen in the plasma density reaches its maximum extent at t = 41 hours (Figure 5c). The inward curvature is clearly visible at this time. An hour later (Figure 5d), the tail has not grown in radial distance and plasma from Titan simply merges into the Kronian magnetospheric plasma. Although the ion tail is several Saturn radii long, it is insufficient to produce a full torus even under the relatively stable conditions during parallel IMF.

4.2. Interaction With Plasma Fingers for Antiparallel IMF

[27] The large-scale view of the system for the antiparallel case is shown in Figure 6. As noted in the introduction, in addition to thinning of the plasma tail, antiparallel IMF can cause the Raleigh-Taylor like interchange instability to become unstable [*Kidder et al.*, 2009]. This instability causes predominantly heavy ions, which originate from the Enceladus ion torus, to move outward while hotter, more tenuous solar wind plasma is drawn inward. These flows lead to discrete "fingers" of cold dense plasma moving outward and hot tenuous plasma moving inward. The cold and dense outwelling fingers are most easily seen in CNO^+ density in Figure 6 as they originate from the Enceladus ion torus but they can also be seen to a lesser extent in H^+ density. Three such fingers are seen developing at t = 64.40 hours, at 1300, 1500, and 2000 SLT. The first of these fingers impacts Titan at 66.40 hours. The second, more intense interchange finger impacts Titan an hour later. The Titan ion tail as seen in the H^+ or Hvy^+ density shows a substantial change in direction as these fingers pass by Titan.

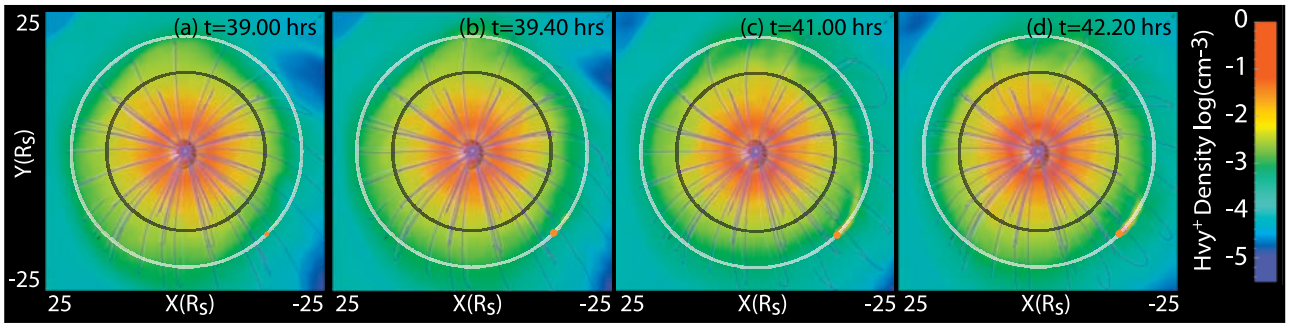

Figure 5. Evolution of the heavy ion density in the equatorial plane on a global scale for the parallel IMF case. In this figure (and subsequent figures except where noted), Titan's position is indicated by an orange dot. The black and white circles indicate positions at r = 14 and 20 R_S, respectively.

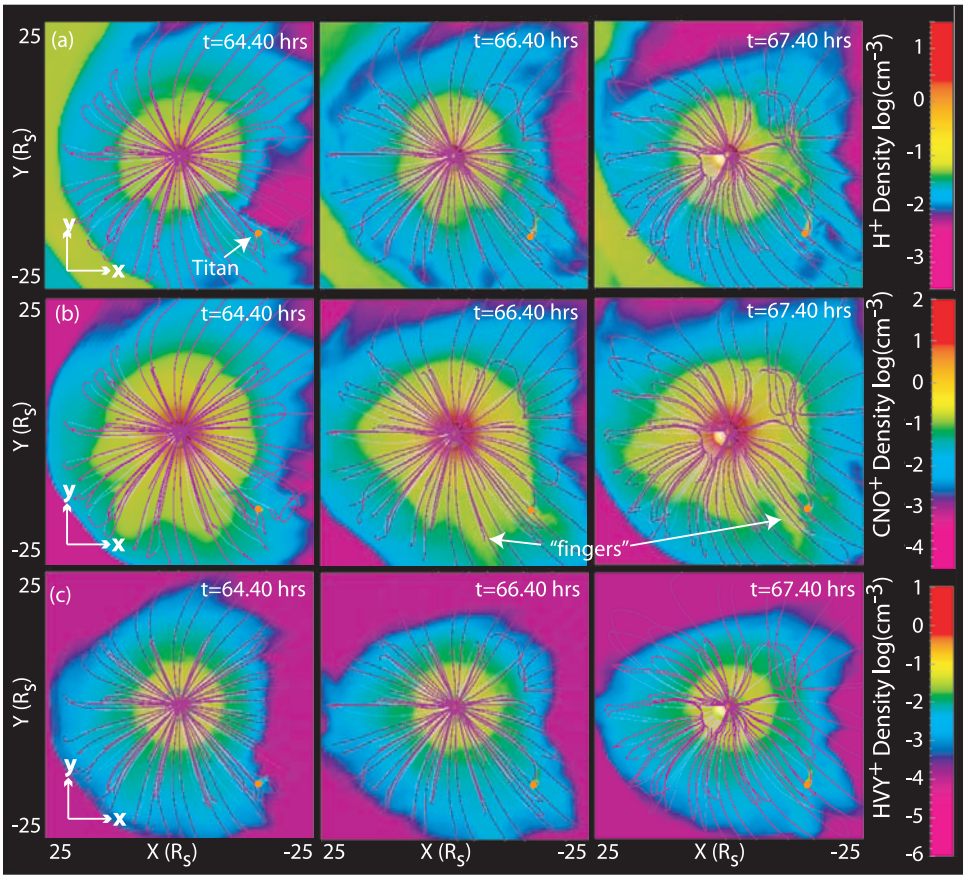

Figure 6. Global equatorial views of proton density, CNO^+ density, and Hvy^+ density for the antiparallel IMF case. The enhanced convection during antiparallel IMF thins Saturn's current sheet and also leads to the enhancement of CNO^+ interchanging fingers outwelling from the inner magnetosphere. Over the time period shown, two such fingers impact Titan and modify the direction and density of Titan's ion tail. The inner edge of the plasma sheet is very close to this interaction region.

[28] The modification of the flow in Titan's ion tail and Saturn's plasma sheet is shown in Figure 7 with a field of view of 16 × 15 R_S. The first interchange finger is seen approaching Titan in Figure 7a. This interaction leads to a void in density and a strong pressure gradient between Titan's tail and the Kronian finger. As the finger propagates around Titan, the Kronian plasma at radial distances beyond Titan attempts to fill this void (Figure 7c). This inward motion changes the flow direction near Titan and causes Titan's tail to be pushed inward (Figures 7c–7f). The density in the tail is enhanced compared to that seen prior to the interaction. The flapping of the tail owing to the variable local environment means a complete torus of Titan plasma is not possible.

[29] Figure 8 shows a 3-D representation of this same interaction. Each interaction leads to a density enhancement in Titan's plasma tail and an alteration of its direction. Interestingly, the interaction also causes the interchange plasma finger to break up, detaching a blob of plasma at t = 66.70 hours and t = 68.00 hours. Note that a disturbance propagates upstream and actually leads to initiation of the breakup of the plasma finger well before it reaches Titan. The detached plasma blob then propagates past Titan.

[30] The fact that a disturbance is seen to propagate upstream is a sign that the interaction is sub-Alfvénic and/or subsonic, allowing a bow wave to form as opposed to being super-Alfvénic where a bow shock would form with no upstream propagation possible. This effect is quantified in Figure 9 which shows the Alfvénic Mach number near Titan for parallel and antiparallel IMF. The top panels show the Mach number before Titan is inserted into the plasma environment and the bottom panels show its evolution approximately 4 hours later. In the parallel case (left-hand side) Titan is initially near the transitional region between super- and sub-Alfvénic flows, and as such is near the inner edge of the plasma disk. The insertion of Titan for the parallel case leads to a reduction in the Mach number in front of Titan as plasma and magnetic field slow due to the interaction with the induced magnetosphere. The minimum in Mach number that is tied to Titan coincides with the position of Titan's ion tail shown in Figure 4. At larger radial distances to Titan there is an increase in Mach number as plasma attempts to fill the void in pressure that Titan's induced magnetosphere causes.

[31] For the antiparallel case (right-hand side) the situation is more complicated. Titan encounters sub- and super-Alfvénic flows associated with the interchange fingers. In such trans-Alfvénic flows (i.e., in transitioning between sub- and super-Alfvénic flows), perturbations are able to propagate both upstream and downstream of Titan, similar

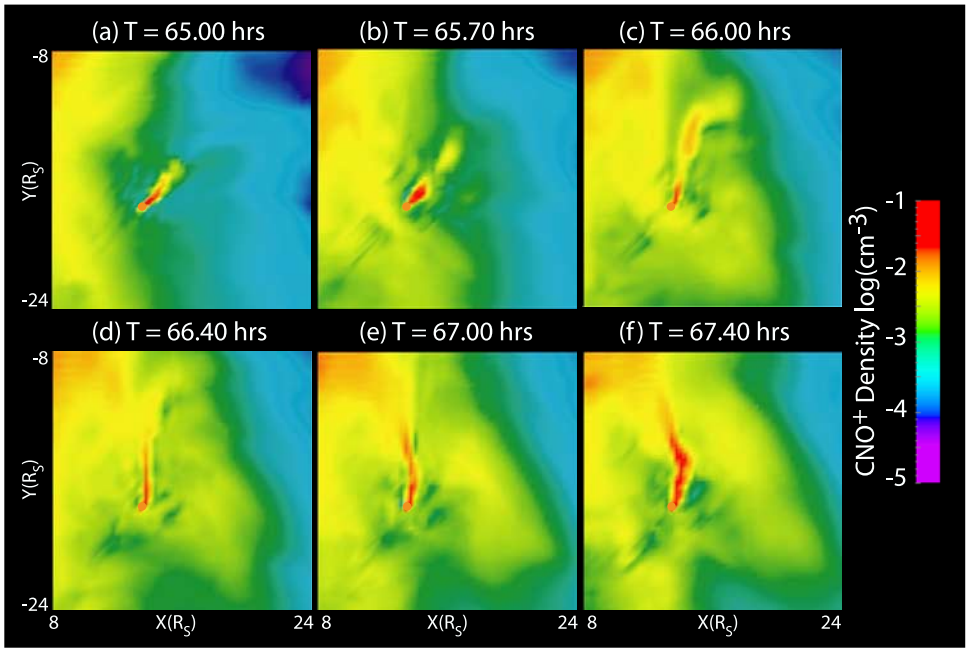

Figure 7. Local view of CNO^+ density corresponding to Figure 6 in the equatorial plane showing Titan's interaction with the first cold, dense interchange finger from Saturn's inner magnetosphere. This interaction warps Titan's ion tail, enhances density in the tail, and breaks up the Kronian interchange finger.

to the parallel case. The minimum in the Alfvén Mach number downstream of Titan coincides with the position of Titan's tail seen in Figures 6 and 7. Similar to the parallel case, the Mach number is higher on the away side of Titan. Since the contours track the flow along Titan's tail and are orthogonal to the initial contours, this increase in Mach number is a response to the interaction with Titan.

5. Titan's Impact on the Kronian Magnetosphere

[32] The above results show that variable conditions within the Kronian magnetosphere clearly modify the properties of Titan's induced magnetosphere. We have also demonstrated that Titan modifies the properties of the plasma interchange fingers. The issue addressed in this section is whether Titan's induced magnetosphere has an impact on the properties of the global Kronian magnetosphere.

[33] The influence of Titan's ion tail on Saturn's magnetic field during parallel IMF is highlighted in Figure 10, which shows B_Z and B_Y in the equatorial plane. Prior to the formation of an extended Titan ion tail, B_Z has a low variation across Titan's orbit. However, by t = 41 hours. (Figure 10c) a large-scale decrease in the strength of $|B_Z|$ is seen across the tail at 20 R_S. The decrease in B_Z is due to the draping of the magnetic field around Titan and Figure 10 gives an indication of the total scale of the draping.

[34] Titan produces measurable perturbations in B_Y as well (Figures 10e–10h), and a depression in B_Y in its wake, which is also associated with the draping of magnetic field. An equally important feature is an enhancement in B_Y ahead of Titan. This enhancement occurs because the interaction at Titan is trans-Alfvénic (Figure 9). As a result, a bow wave forms instead of a bow shock and magnetic disturbances are able to propagate in front of Titan. The full bow wave at 0200 SLT illustrates the importance of incorporating local and global effects into one model.

[35] The global impact of Titan on Saturn's plasma sheet is further illustrated in Figure 11, which shows the proton density in the noon-midnight meridian during parallel IMF. At early times the tail density decreases monotonically with radial distance (Figures 11a and 11b). At t = 41 hours there is a localization of density near Titan's orbit, which is seen to extend over z ± 3 R_S, causing the sheet to appear thicker just beyond Titans' orbit than at the two earlier times. At the last time the plasma sheet appears closer to the equatorial than at the beginning of the simulations.

[36] In order to demonstrate more clearly any change in the position of the plasma sheet, Figure 12 shows contours of the magnetic field strength in a cut along the noon-midnight meridian. The contouring is saturated within the inner magnetosphere, so that the middle magnetospheric fields are seen more easily. Saturn's magnetic field is known to form a magnetodisc outside of ~18 R_S because the current sheet outside of this distance is extended owing to centrifugal stress. This force causes the field lines to become stretched and flattens them into a disk [*Arridge et al.*, 2007]. This may be seen in Figure 12a where the magnetodisc is very bowl-shaped and the tail region arches strongly upward. By 42.40 hours, mass loading from Titan has pulled the magnetodisc down and closer to the equatorial plane, consistent with the density plots in Figure 11. *Arridge et al.* [2007], estimated the total mass of the magnetodisc (plasma in the torus from 18 to 45 R_S) to be 10^6 kg. Titan is increasing the mass of a localized (<1 R_S) region of the magnetodisc by about 100 kg/hour so it is

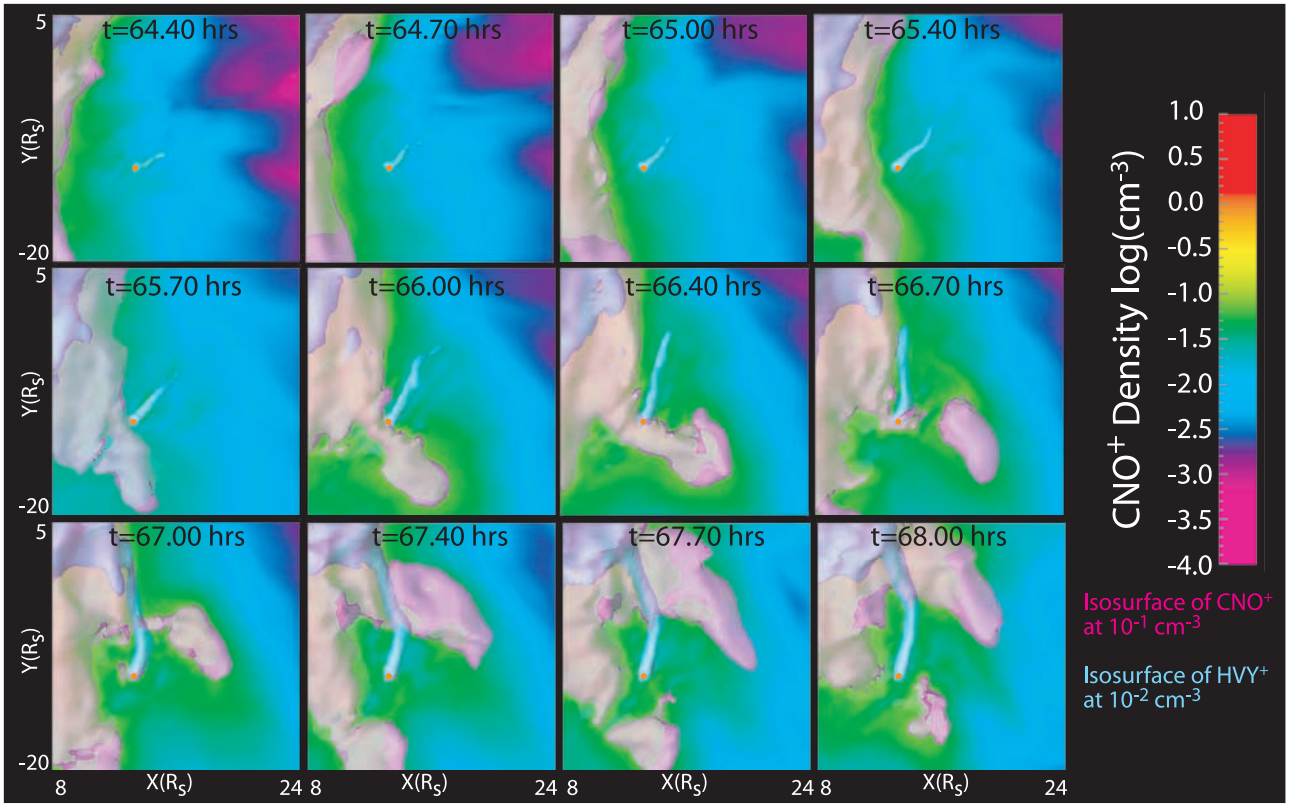

Figure 8. A 3-D view of the interaction between Titan and the first and second interchange fingers. The blue surface is a surface of constant Hvy^+ density (10^{-2} cm^{-3}). This surface emphasizes Titan's ion tail. The color mapping shows the density of the CNO^+ in the equatorial plane. The magenta surface is to emphasize the plasma fingers and is a surface of constant CNO^+ density (10^{-1} cm^{-3}). The enhanced outflow produced by the first interaction is sufficient for Titan to totally disrupt the second finger. This latter interaction starts to occur prior to Titan's actual immersion in the finger.

conceivable that Titan can have a large effect over nearly 4 hours.

[37] For the antiparallel case, it is evident that the plasma sheet is much thinner relative to the parallel case. Figure 12 illustrates the close proximity between Titan's tail and the inner edge of the current sheet (seen as an abrupt decrease in magnetic field strength and the contours are no longer bent). The mass loading from Titan which is a factor of 5 higher than the parallel case does not change the position of the magnetodisc as much as in the parallel case. Nevertheless, it may have a significant role in the Kronian dynamics as it lies very close to the inner edge of the plasma sheet (as seen by the sharp gradient in $|B|$). For example at t = 64.40 hours the inner edge of the current sheet is above Titan, whereas at t = 67.40 hours the inner edge is at the same height as Titan. It is not known how much of this shift is due to Titan and how much is due to effects arising from the thinning of the current sheet under antiparallel IMF.

[38] Another way to see the position of the inner edge of the plasma sheet is via a transition from cold, dense plasma from the inner magnetosphere to hot, tenuous plasma. Figure 13 shows this transition for parallel and antiparallel IMF. During parallel IMF, this boundary is well within the orbit of Titan and the growth of Titan's ion tail has little effect on the flows near this boundary. However, for the antiparallel case this boundary is much closer to Titan's orbit because the interchange instability causes the cold inner magnetospheric plasma to move farther out on average [*Kidder et al.*, 2009]. For this case, Titan has the potential to modify the properties of the inner edge of the plasma sheet.

[39] This effect is illustrated in Figure 14 by a series of cuts in the CNO^+ density in (1) the equatorial plane showing the arrival of an interchange finger similar to the previous figures but at higher resolution and (2) in the vertical plane in front of, through, and behind Titan. The vertical cuts are taken in a direction approximately orthogonal to the initial flow direction. It is seen that Titan is able to produce a void in the plasma density (or plasma depletion) across the entire vertical width of the plasma finger (i.e., Figures 14c and 14d) out to $\sim$2 R_S in the downstream region of Titan. There is no such void in the upstream region which indicates that the void/depletion region is a Titan effect. This broad interaction arises from the draping of Kronian magnetic field over Titan's ion tail.

[40] The void has a large effect on the radial flows near Titan and leads to the tail flapping previously discussed. Another way to see the effect of the void is through the changes in velocity in the vicinity of Titan as shown in Figure 15. Before Titan is inserted into the simulation, cold plasma flowing on the dusk side is convected down the tail similar to the Vasyliunas circulation model [*Vasyliunas*,

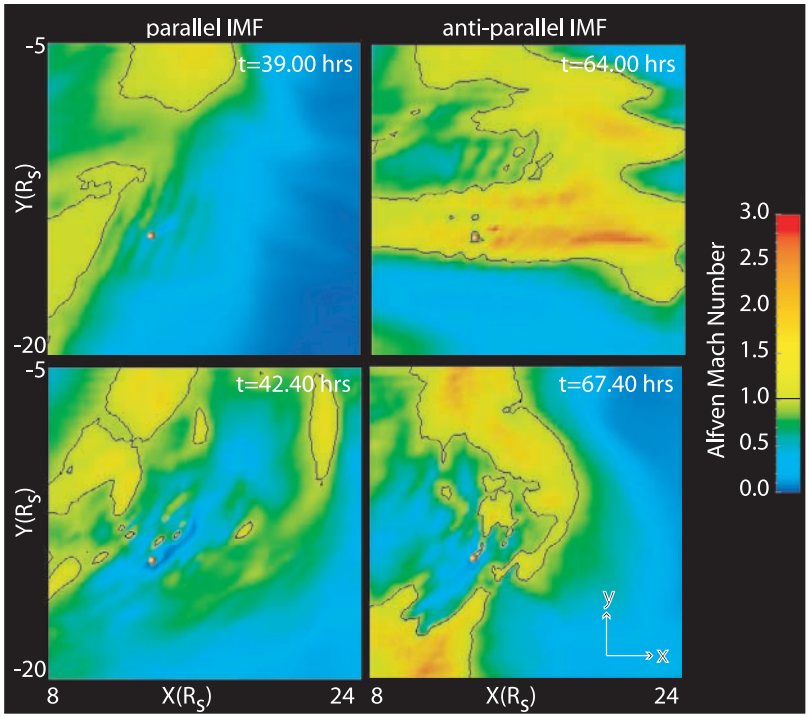

Figure 9. Equatorial contours of the Alfvénic Mach number in the vicinity of Titan. For the parallel IMD case, Titan lines initially near a trans-Alfvénic region, but Titan's influence leads to region of sub-Alfvénic speed both in front of and behind Titan. For the antiparallel case, higher-speed flows are initially present, but Titan's influence again leads to sub-Alfvénic speeds both in front of and behind Titan.

1983]. In the presence of Titan, a portion of this plasma now flows toward Saturn (Figure 15b) and the size of this region increases within time (Figure 15c). So, while Titan's ion tail is influenced by convective flows associated with Saturn's plasma sheet, the reverse is also true, that is that the flow in the plasma sheet is modified by Titan's ion tail.

[41] The corresponding temperature plots in Figure 16 indicate that the density void produced by Titan is filled with hotter plasma that is typically associated with an outer

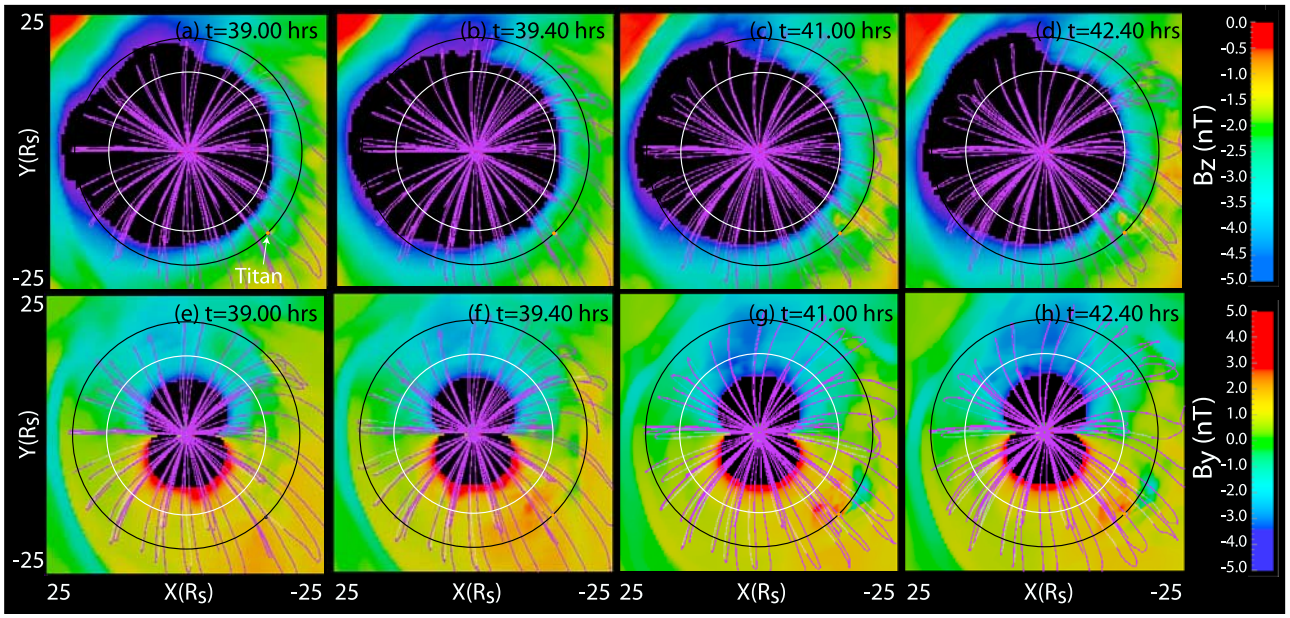

Figure 10. Evolution of (top panels) B_Z and (bottom panels) B_Y corresponding to Figure 5. Titan is shown as a black dot. Pileup of B_Z occurs coincident with Titan's plasma tail, while the B_Y contours show propagation of the disturbance upstream of Titan because the interaction with Titan is sub-Alfvénic.

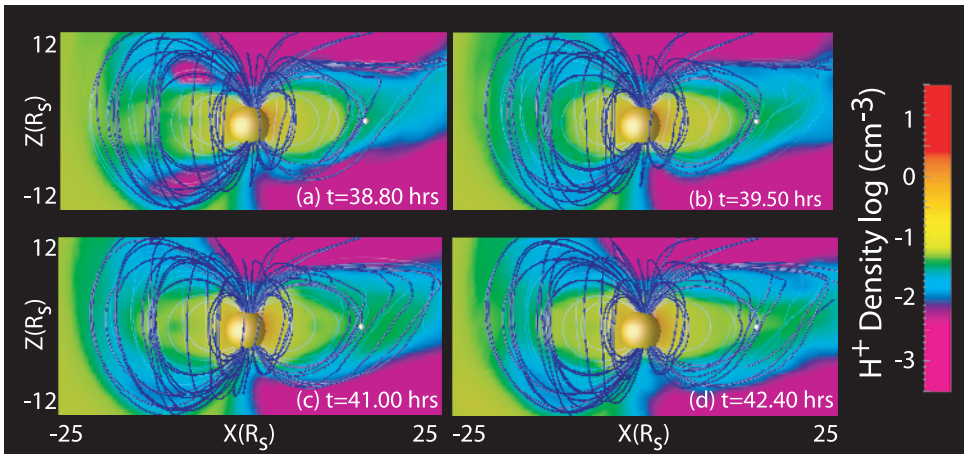

Figure 11. Contours of the noon-midnight meridian density of the protons for parallel IMF. The interaction with Titan causes less bending of the plasma disk and a pileup of light ions at Titans radial distance that extends over z $\sim \pm 3\ R_S$.

magnetospheric source, as opposed to the colder plasma from Titan or the Kronian inner magnetosphere. This filling in by hot plasma is consistent with the previous figure where middle magnetospheric plasma that is hot and tenuous is seen to flow inward.

[42] This result lends itself to an interesting speculation. As noted in the introduction, the occurrence of SKR

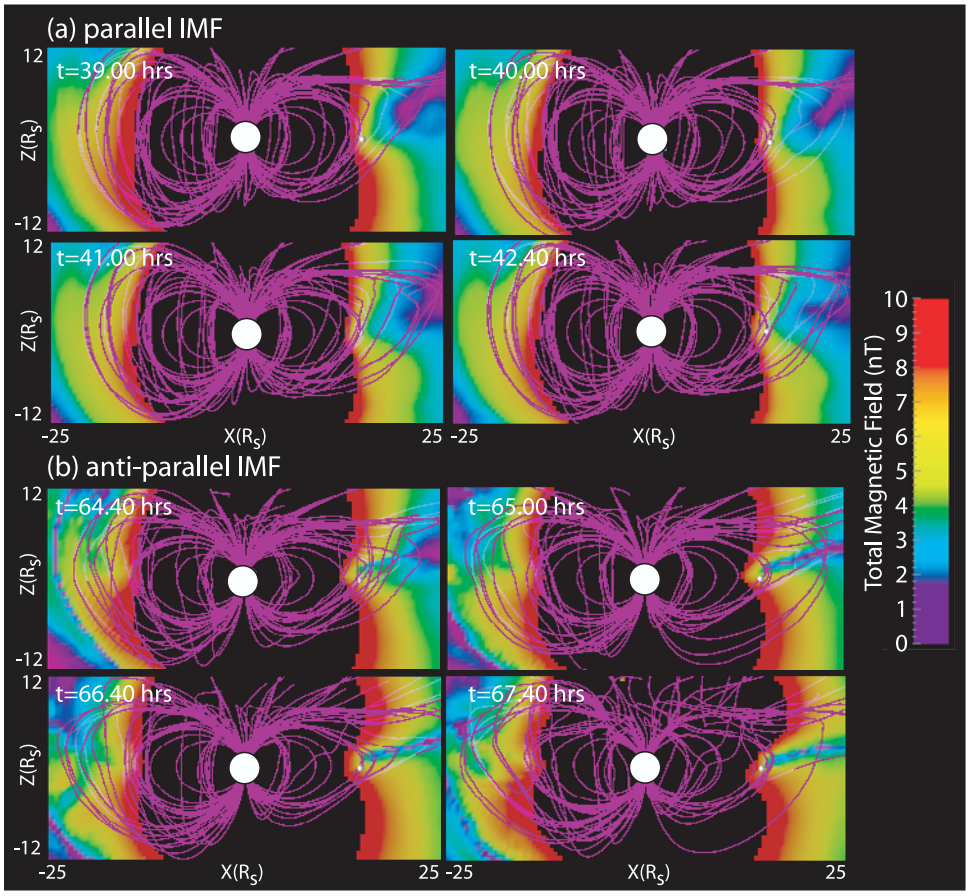

Figure 12. Total magnetic field in the noon-midnight meridian for (a) parallel IMF and (b) antiparallel IMF. Mass loading from Titan forces the magnetodisk to have less of a bowl shape during parallel IMF. Titan's does not have as large an effect during antiparallel IMF owing to the external forcing of the interplanetary field.

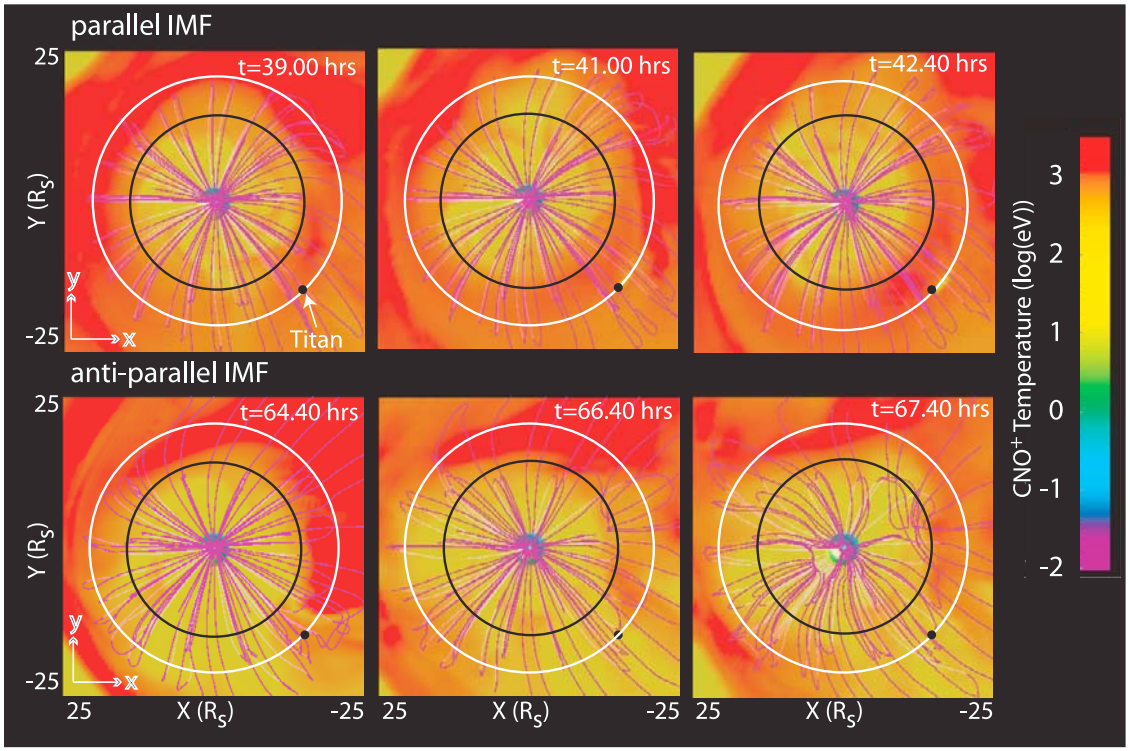

Figure 13. Global equatorial view of CNO^+ temperature for (top) parallel IMF and (bottom) antiparallel IMF. In the case of parallel IMF the transition from hot to cold plasma, representing the edge of the plasma sheet, occurs well within Titan's orbit, and Titan does not have a large influence on this boundary. The inner plasma sheet boundary is nearly coincident with Titan in the antiparallel case, and Titan is able to affect the flows near this boundary on a large scale.

increases when Titan is in Saturn's tail [*Menietti et al.*, 2007]. SKR preferentially occurs in magnetized regions with low densities where there are semirelativistic electrons present [*Wu and Lee*, 1979]. In its present position in the model, Titan blocks the inward flow of the plasma sheet, leading to plasma depletions, with keV electrons being present. Flow of this hot, tenuous plasma into the auroral regions would produce conditions favorable for the generation of SKR. We can only speculate that this could be the cause of enhanced SKR, since the model does not incorporate full electron dynamics.

6. Conclusions

[43] In this paper we present the first simulations of the interaction between Titan's induced magnetosphere coupled with the global Kronian magnetosphere. The treatment of this coupled system is difficult, owing to the disparate spatial and temporal scales and multiple sources of plasma composed of different ions. To tackle these problems we have used a model that is both multifluid and multiscale. The multifluid aspect of the model allows for the self-consistent incorporation of solar wind protons, Saturn ionospheric plasma, ions from an Enceladus torus, and ions from Titan's ionosphere. The latter two sources have significant components of heavy ions including CNO^+, as well as heavy ions including N_2^+, O_2^+ and organic ions. The model incorporates these different ion species by separately tracking the transport of three ion populations: (1) protons, (2) CNO^+ (assumed to have a mass of 16 amu), and (3) Hvy^+ (assumed to have a mass of 32 amu). Global dynamics are established by first running the magnetospheric simulations with resolution of 0.25 R_S for a few tens of hours of real time and by establishing an equilibrium for Saturn's magnetosphere under the influence of different IMF conditions. Titan's interaction with Saturn's magnetosphere is then examined using refinement gridding to resolve spatial scales down to ~100 km near Titan.

[44] In this paper we have examined the coupled interactions when Titan is in the premidnight sector, allowing us to investigate the transport of Titan's plasma into the Kronian plasma sheet. Two IMF configurations are considered: IMF parallel and antiparallel to the planetary field. For parallel IMF the dynamics of the Kronian magnetosphere are relatively quiet with a thick Kronian plasma sheet. Because Saturn's rotation and magnetic equators are not in the ecliptic plane, the influence of the solar wind creates a bowl shape to the magnetosphere [e.g., *Arridge et al.*, 2007]. When Titan is in the premidnight sector, plasma outflow from Titan produces sufficient mass loading that the plasma sheet stays in the magnetic equator at least out to Titan's orbit, so that Titan has a global effect on Saturn's magnetosphere. Titan's ion tail is stable for this configuration with little change in its flow direction for the several hours of real time in the simulations. Titan's ion tail extends 10 R_S in length, yet moves slower than corotation, and is seen to bend inward toward Saturn, and is unable to form a complete torus.

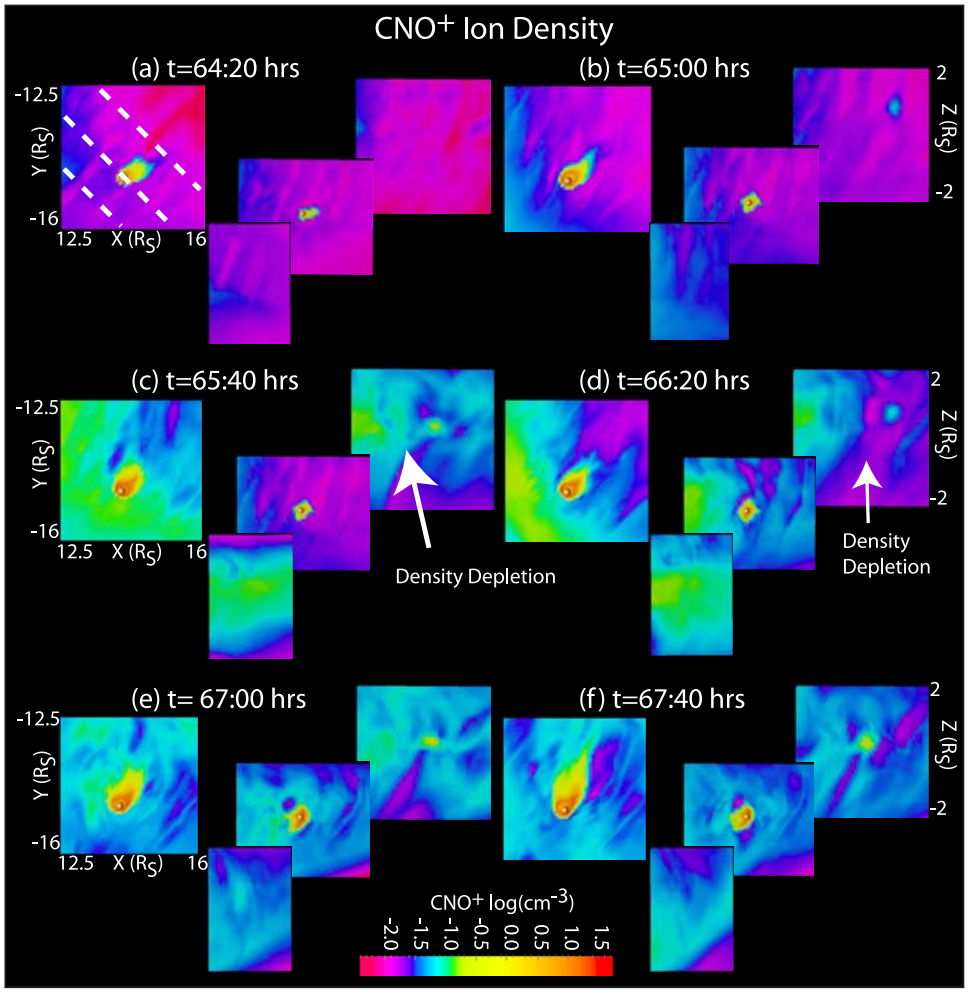

Figure 14. Close-up of the evolution of CNO^+ density. In each set the flat panel shows the density in the equatorial plane. The vertical panels show cuts approximately orthogonal to the incident flow in the vertical direction (in front of Titan, through Titan, and behind Titan). The positions of these cuts are indicated by the dashed white lines in Figure 14a. Titan's interaction leaves a void in density behind the moon that spans the entire width of the plasma sheet.

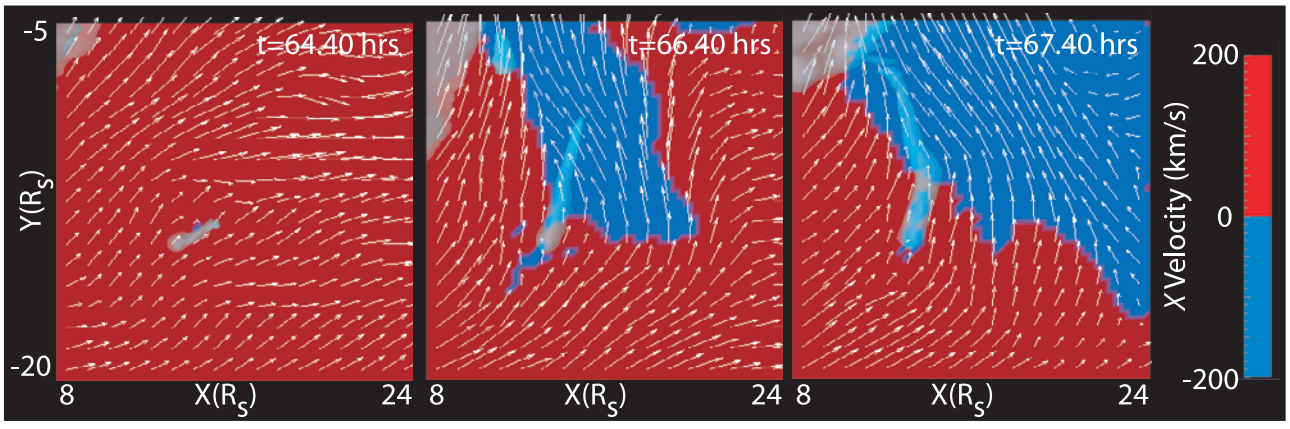

Figure 15. Equatorial CNO^+ velocity in the x-direction mapped using arrows and color mapping. Over 3 hours, Titan's interaction with the local plasma environment changes the large-scale flow in the region directly behind Titan.

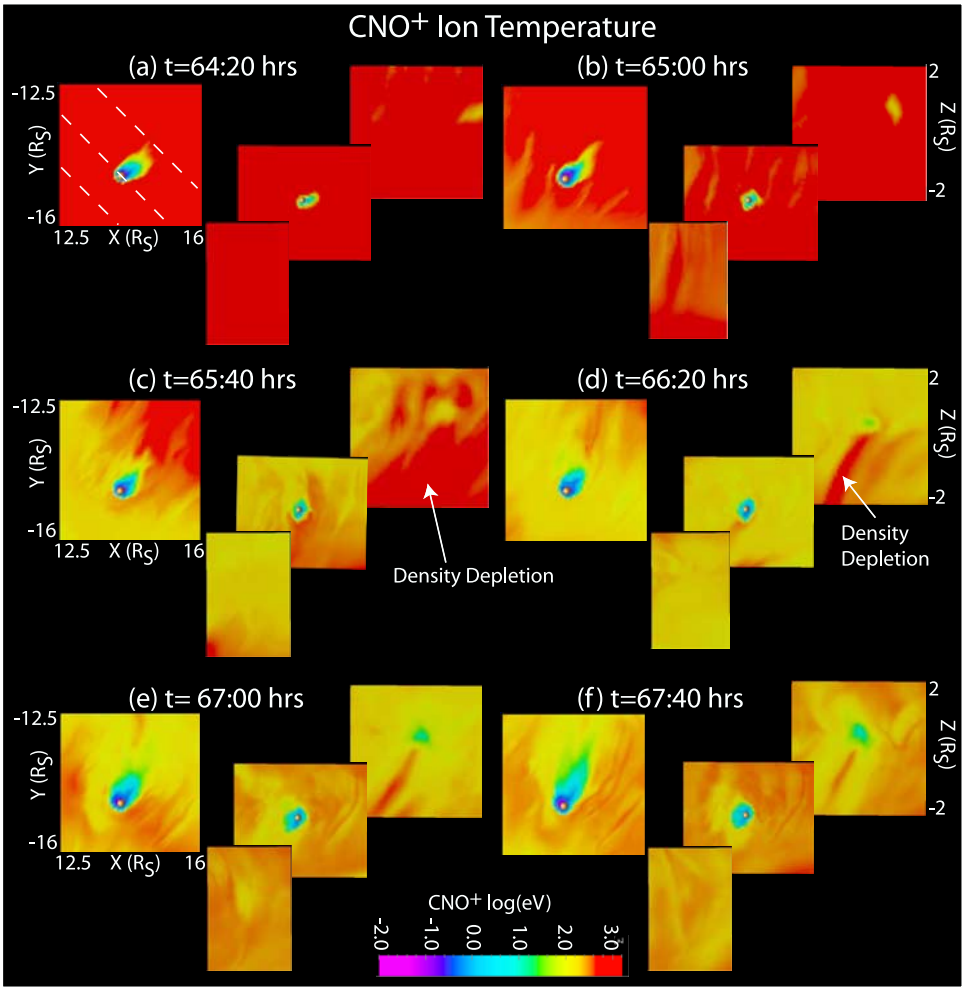

Figure 16. Same configuration as in Figure 14, but showing CNO^+ temperature. The density depletion discussed in Figure 12 is seen to have an elevated temperature.

[45] For antiparallel IMF the situation is more dynamic. Titan's outflow rate for the same initial conditions at Titan is seen to increase from 3 to 4 $\times$ 10^{24} ions/s for parallel IMF to 1.2 $\times$ 10^{25} ions/s for antiparallel IMF. The flux of heavy ions increases faster than that of the light ions so that for antiparallel IMF the composition changes from an outflow dominated by light ions to one that has nearly equal fluxes of light and heavy ions.

[46] Another difference for antiparallel IMF is that enhanced convection within the inner magnetosphere causes the centrifugal interchange instability to become unstable. This instability leads to the formation of discrete plasma fingers, transporting cold dense ions from Enceladus outward and hot tenuous Kronian plasma inward. Titan's ion tail interacts with these interchange fingers, modifying the dynamics of both magnetospheres. Titan is able to disrupt, or breakup the motion of the fingers leading to the generation of discrete plasma blobs. This disruption occurs in front of Titan since the interaction is sub-Alfvénic.

[47] In the wake of this interaction, a plasma void develops. Plasma from larger radial distances moves in to fill this void. As this plasma flows in, it pushes onto Titan's plasma tail. This interaction alters the direction of Titan's tail, swinging it inward by as much as 45° so that the tail is transported closer toward Saturn than for parallel IMF (of the order of a few Saturn radii). This flapping of Titan's ion tail impedes the formation of a complete torus at Titan's orbit so that in both cases a complete torus cannot be formed.

[48] Because of the interaction with the interchange fingers, Titan's ion tail coincides with the inner edge of the plasma sheet. An important feature of the interactions is the draping of Saturn's magnetic field along Titan's tail. This draping produces a barrier across the entire vertical width of the Kronian plasma sheet even though Titan's ion tail is much smaller than the total width of the plasma sheet. The barrier appears as a depleted plasma density, which is filled with hot tenuous magnetospheric plasma.

[49] The above results show that there can be dramatic changes in Saturn's magnetospheric dynamics and Titan's induced magnetosphere when they are treated as a coupled system. New effects include: a change in the position of Saturn's plasma sheet relative to the magnetic equator, a change in the position of the inner edge of Saturn's plasma sheet, and variable flux and direction of Titan's ion tail.

[50] Our results hint at a possible explanation for an apparent enhancement of SKR when Titan is in the nightside, as indicated by *Menietti et al.* [2007]. Titan's ion tail is

able to modify the position of the inner boundary of the plasma sheet and in so doing may modify the processes associated with substorm activity and aurorae. In addition, Titan's ion tail acts as a barrier to the magnetospheric flows and creates tenuous regions of hot plasma which aide in the creation of conditions that favor SKR.

[51] At this time we have only considered Titan in one position along its orbit. Future work will be undertaken to determine how Titan might affect Saturn's magnetospheric dynamics in other SLT positions, specifically when Titan is near the dayside magnetopause.

[52] **Acknowledgments.** This work was supported by NASA grants NNX07AJ80G and NNX08AR16G and the NSF Astrobiology Program at the University of Washington.

[53] Amitava Bhattacharjee thanks Andreas Kopp and another reviewer for their assistance in evaluating this paper.

References

Arridge, C. S., C. T. Russell, K. Khurana, N. Achilleos, N. André, A. M. Rymer, M. K. Dougherty, and A. J. Coates (2007), Mass of Saturn's magnetodisc: Cassini observations, *Geophys. Res. Lett.*, *34*, L09108, doi:10.1029/2006GL028921.

Blanc, M., et al. (2002), Magnetospheric and plasma science with Cassini-Huygens, *Space Sci. Rev.*, *104*, 253–346, doi:10.1023/A:1023605110711.

Brecht, S. H., J. G. Luhmann, and D. J. Larson (2000), Simulation of the Saturnian magnetospheric interaction with Titan, *J. Geophys. Res.*, *105*, 13,119–13,130, doi:10.1029/1999JA900490.

Crary, J. F., et al. (2005), Solar wind dynamic pressure and electric field as the main factors controlling Saturn's aurorae, *Nature*, *433*, 720–722, doi:10.1038/nature03333.

Cravens, T. E. (2005), Titan's ionosphere: Model comparisons with the Cassini Ta data, *Geophys. Res. Lett.*, *32*, L12108, doi:10.1029/2005GL023249.

Dougherty, M. K., et al. (2005), Cassini magnetometer observations during Saturn Orbit Insertion, *Science*, *307*, 1266–1270, doi:10.1126/science.1106098.

Hansen, K. C., T. I. Gombosi, D. L. DeZeeuw, C. P. T. Groth, and K. G. Powell (2000), A 3D global MHD simulation of Saturn's magnetosphere, *Adv. Space Res.*, *26*, 1681–1690, doi:10.1016/S0273-1177(00)00078-8.

Hansen, K. C., A. J. Ridley, G. B. Hospodarsky, N. Achilleous, M. K. Dougherty, T. I. Gombosi, and G. Toth (2005), Global MHD simulations of Saturn's magnetosphere at the time of the Cassini approach, *Geophys. Res. Lett.*, *32*, L20S06, doi:10.1029/2005GL022835.

Harnett, E. M., and R. M. Winglee (2003), The influence of a mini-magnetopause on the magnetic pileup boundary at Mars, *Geophys. Res. Lett.*, *30*(20), 2074, doi:10.1029/2003GL017852.

Harnett, E. M., and R. M. Winglee (2007), High-resolution multifluid simulations of the plasma environment near the Martian magnetic anomalies, *J. Geophys. Res.*, *112*, A05207, doi:10.1029/2006JA012001.

Harnett, E. M., R. M. Winglee, and P. A. Delamere (2005), Three-dimensional multi-fluid simulations of Pluto's magnetosphere: A comparison to 3D hybrid simulations, *Geophys. Res. Lett.*, *32*, L19104, doi:10.1029/2005GL023178.

Hendricks, S., F. M. Neubauer, M. K. Dougherty, N. Achilleos, and C. T. Russell (2005), Variability of Saturn's bow shock and magnetopause from Pioneer and Voyager: Probabilistic predictions and initial observations by Cassini, *Geophys. Res. Lett.*, *32*, L20S08, doi:10.1029/2005GL022569.

Kidder, A., R. M. Winglee, and E. M. Harnett (2009), Regulation of the centrifugal interchange cycle in Saturn's inner magnetosphere, *J. Geophys. Res.*, *114*, A02205, doi:10.1029/2008JA013100.

Kopp, A., and W. H. Ip (2001), Asymmetric mass loading effect at Titan's ionosphere, *J. Geophys. Res.*, *106*, 8323–8332, doi:10.1029/2000JA900140.

Krupp, N. (2005), Energetic particles in the magnetosphere of Saturn and a Comparison with Jupiter, *Space Sci. Rev.*, *116*, 345–369, doi:10.1007/s11214-005-1961-3.

Ledvina, S. A., S. H. Brecht, and J. G. Luhmann (2004), Ion distributions of 14 amu pickup ions associated with Titan's plasma interaction, *Geophys. Res. Lett.*, *31*, L17S10, doi:10.1029/2004GL019861.

Ma, Y.-J., A. F. Nagy, T. E. Cravens, I. V. Sokolov, J. Clark, and K. C. Hansen (2004), 3-D global MHD model prediction for the first close flyby of Titan by Cassini, *Geophys. Res. Lett.*, *31*, L22803, doi:10.1029/2004GL021215.

Menietti, J. D., J. B. Groene, T. F. Averkamp, G. B. Hospodarsky, W. S. Kurth, D. A. Gurnett, and P. Zarka (2007), Influence of Saturnian moons on Saturn kilometric radiation, *J. Geophys. Res.*, *112*, A08211, doi:10.1029/2007JA012331.

Nagy, A. F., et al. (2001), The interaction between the magnetosphere of Saturn and Titan's ionosphere, *J. Geophys. Res.*, *106*, 6151–6160, doi:10.1029/2000JA000183.

Paty, C., and R. M. Winglee (2004), Multi-fluid simulations of Ganymede's magnetosphere, *Geophys. Res. Lett.*, *31*, L24806, doi:10.1029/2004GL021220.

Paty, C., and R. M. Winglee (2006), The role of ion cyclotron motion at Ganymede: Magnetic field morphology and magnetospheric dynamics, *Geophys. Res. Lett.*, *33*, L10106, doi:10.1029/2005GL025273.

Simon, S., et al. (2007), Three-dimensional multi-species hybrid simulations of Titan's highly variable plasma environment, *Ann. Geophys.*, *25*, 117–144.

Snowden, D., R. Winglee, C. Bertucci, and M. Dougherty (2007), Three-dimensional multifluid simulation of the plasma interaction at Titan, *J. Geophys. Res.*, *112*, A12221, doi:10.1029/2007JA012393.

Vasyliunas, V. M. (1983), Comparative magnetospheres, in *Solar-Terrestrial Physics, Principles and Theoretical Foundations*, pp. 479–492, Max-Planck-Inst. für Aeron, Katlenburg-Lindau, Germany.

Wahlund, J.-E., et al. (2005), Cassini measurements of cold plasma in the ionosphere of Titan, *Science*, *308*, 986–989, doi:10.1126/science.1109807.

Winglee, R. M. (1998), Multi-fluid simulations of the magnetosphere: The identification of the geopause and its variation with IMF, *Geophys. Res. Lett.*, *25*, 4441–4444, doi:10.1029/1998GL900217.

Winglee, R. M. (2000), Mapping of ionospheric outflows into the magnetosphere for varying IMF conditions, *Sol. Terr. Phys.*, *62*, 527–540, doi:10.1016/S1364-6826(00)00015-8.

Winglee, R. M. (2004), Ion cyclotron and heavy ion effects on reconnection in a global magnetotail, *J. Geophys. Res.*, *109*, A09206, doi:10.1029/2004JA010385.

Wu, C. S., and L. C. Lee (1979), Theory of the terrestrial kilometric radiation, *Astrophys. J.*, *230*, 621–626, doi:10.1086/157120.

Young, D. T., et al. (2005), Composition and dynamics of plasma in Saturn's magnetosphere, *Science*, *307*, 1262–1266, doi:10.1126/science.1106151.

A. Kidder, D. Snowden, and R. M. Winglee, Department of Earth and Space Science, University of Washington, Box 351310, Seattle, WA 98195, USA. (winglee@ess.washington.edu)